ZANCO Journal of Pure and Applied Sciences

TYPE Original article
DOI http://dx.doi.org/10.21271/ZJPAS.38.2.5

OPEN ACCESS

*Corresponding author

Sumaya I. Ahmed
sumaya.ahmad@soran.edu.iq

RECEIVED:04 /06 /2025
ACCEPTED :24/09/ 2025
PUBLISHED:30/ 04/ 2026

KEYWORDS:

Multidrug resistant, Pseudomonas aeruginosa, Green silver nanoparticle, Glycyrrhiza glabra root, Antibiofilm.

Green Synthesis of Silver Nanoparticles Using Glycyrrhiza glabra Root Extract for Antibacterial and Antibiofilm Activity Against Multidrug-*Resistant Pseudomonas aeruginosa* Clinical Isolates

Sumaya I. Ahmed [1] and Abdulkarim Y. Karim [2]

1 Department of Biology, College of science,Soran University, Soran, Iraq.
2Department of Biology, College of science,Salahaddin University, Erbil, Iraq.

ABSTRACT

Background: *Pseudomonas aeruginosa* is an opportunistic pathogen that contributes to treatment failure due to its strong biofilm-forming ability and multidrug resistance (MDR). This study intended to assess the antibacterial and antibiofilm properties of silver nanoparticles (AgNPs) synthesized from *Glycyrrhiza glabra* root extract against MDR-*P. aeruginosa* clinical isolates.
Methods: 128 clinical specimens were collected from patients who were receiving medical care in Erbil, Kurdistan Region, Iraq. Clinical specimens were cultured and analyzed using standard biochemical tests to identify *P. aeruginosa*. Antibiotic susceptibility testing was performed for identify MDR isolate. Biofilm production was evaluated with a microtiter plate technique through safranin staining. AgNPs were synthesized from an aqueous extract of *G. glabra* root. The antibacterial activity was assessed by a well diffusion test, and the Minimum Inhibitory Concentration (MIC) and Minimum Bactericidal Concentration (MBC) were determined using microdilution in 96-well plates. AgNPs were tested for their capacity to inhibit and eradicate biofilms.
Results: Thirty-four (26.6%) isolates were identified as *P. aeruginosa*, of which 26 (76.5%) exhibited MDR. Among these MDR isolates, 80.7% exhibited robust biofilm formation, 11.5% moderate, 3.8% weak, and 3.8% produced no biofilm. AgNPs demonstrated inhibition zones measuring 17 mm in 1500 µg/mL, and MIC values between 62.5 and 500 µg/mL. At a concentration of 500 µg/mL, AgNPs exhibited 97% biofilm inhibition and 85% eradication.
Conclusion: AgNPs derived from *G. glabra* root extract shown significant antibacterial and antibiofilm properties against MDR-*P. aeruginosa* isolates. These findings demonstrate their potential as alternative therapeutic agents for the management of MDR-*P. aeruginosa* infections.

1. Introduction

Pseudomonas aeruginosa is a Gram-negative, opportunistic pathogen widely distributed in nature and responsible for both community- and hospital-acquired infections, including urinary tract infections, pneumonia, and bacteremia. It is particularly problematic in immunocompromised patients and those with burns, surgical wounds, or chronic infections (Azam and Khan, 2019, Abdulhaq et al., 2020). Due to frequent and prolonged antibiotic exposure, *P. aeruginosa* readily develops resistance to multiple drug classes, posing significant therapeutic challenges (Fernebro, 2011). This resistance is largely attributed to its intrinsic defense mechanisms, including efflux pumps and quorum sensing systems, which regulate the expression of virulence factors such as pyocyanin, proteases, and biofilm formation (Antunes et al., 2010, Brindhadevi et al., 2020).

Biofilm formation is a key survival strategy of *P. aeruginosa*, enabling chronic colonization of tissues and resistance to both antibiotics and host immune responses (Thi et al., 2020, Tuon et al., 2022). Biofilms are complex microbial communities embedded in a self-produced extracellular matrix composed of exopolysaccharides, proteins, extracellular DNA, and amyloids. This matrix acts as a physical and chemical barrier, reducing antibiotic penetration and creating microenvironments that can increase resistance up to 1000-fold (Hetta et al., 2023, Afrasiabi and Partoazar, 2024).

Conventional antibiotics often fail to eradicate biofilms, highlighting the urgent need for novel therapeutic approaches (Khan et al., 2021). Nanotechnology offers an attractive method for combating microbial diseases, especially via the application of metallic nanoparticles. AgNPs are distinguished by their broad-spectrum antibacterial activity and better efficacy at lower MIC in comparison to other nanoparticles, including zinc oxide (ZnO), copper oxide (CuO), and gold (AuNPs). Their nanoscale dimensions (1–100 nm) provide an adequate surface area-to-volume ratio, facilitating efficient contact with bacterial membranes, disruption of cellular activities, and production of reactive oxygen species. AgNPs demonstrate significant efficacy against several pathogens, including *Enterococcus faecium, Staphylococcus aureus, Klebsiella pneumoniae, Acinetobacter baumannii, Pseudomonas aeruginosa, and Enterobacter* species (ESKAPE) species and biofilm-associated bacteria (Makabenta et al., 2021, Mikhailova, 2025, Gusso et al., 2025). Importantly, AgNPs can penetrate biofilm matrices and inhibit bacterial growth and biofilm formation (Rajivgandhi et al., 2020).

In recent years, green synthesis methods for AgNPs production have gained attention due to their eco-friendliness, low cost, and biocompatibility. *G. glabra* (licorice), a member of the Fabaceae family, is rich in bioactive compounds such as flavonoids, saponins, glycosides, and phenolics that can act as natural reducing and capping agents in nanoparticle synthesis, the main active component, glycyrrhizin, contributes to the plant's therapeutic potential (Pastorino et al., 2018, Wu et al., 2024).

The present study aims to synthesize silver nanoparticles using *G. glabra* root extract and evaluate their antibacterial and antibiofilm activity against multidrug-resistant clinical isolates of *P. aeruginosa.*

2.Materials and Methods

2.1. Sample Collection

A total of 128 Clinical specimens, including burns, wounds, ear discharge, urine, and sputum, were collected between 15th October and 1st December 2024 from patients attending four hospitals in Erbil, Kurdistan Region, Iraq: Ashti, Emergency, Nanakaly, and Rizgary. The study included 59 male patients (46.1%), and 69 female patients (53.9%) female patients ranging in age from 10 months to 91 years.

2.2. Isolation and Identification of P. aeruginosa

Each sample was immediately inoculated onto sterile cetrimide agar and incubated at 37 °C for 24 hours. Colonies were identified as *P. aeruginosa* based on colony morphology, Gram staining, oxidase test, and confirmation using the VITEK2 system. Isolates were preserved in nutrient broth supplemented with 20% glycerol and stored at –80 °C for further analysis.

2.3. Antimicrobial Susceptibility Testing

The antibiotic susceptibility of the isolates was evaluated using the Kirby-Bauer disk diffusion method on Mueller–Hinton agar (Bauer et al., 1966). Overnight cultures were adjusted to 0.5 McFarland standard and inoculated onto agar plates. After placing the antibiotic discs, plates were incubated at 37 °C for 24 hours. The inhibition zones were measured and interpreted according to (Clinical and Laboratory Standards Institute, 2020) guidelines. The tested antibiotics included: Amikacin (30 µg), Tobramycin (10 µg), Gentamicin (10 µg), Ceftazidime (30 µg), Aztreonam (30 µg), Ciprofloxacin (5 µg), Piperacillin–Tazobactam (100/10 µg), Imipenem (10 µg), Meropenem (10 µg), Cefotaxime (30 µg), and Doxycycline (30 µg) (Magiorakos et al., 2012).

2.4. Biofilm Formation Assay

Biofilm formation was assessed using the 96-well microtiter plate method (Chimi et al., 2024). Overnight cultures were diluted in nutrient broth containing 0.5% glucose. A 200 µL aliquot of each bacterial suspension was transferred into a sterile, flat-bottomed 96-well polystyrene microplate and incubated at 37 °C for 48 hours. Wells were then washed three times with PBS (pH 7.4), air dried at 37 °C, and stained with 0.1% safranin for 15 minutes. Excess stain was washed off with PBS and the plates were dried. Bound dye was solubilized with 200 µL of 96% ethanol, and absorbance was measured at 492 nm using an ELISA reader (Das et al., 2016).

Biofilm formation was categorized based on the OD values relative to the cut-off OD (ODc = average OD of negative control + 3× Standard deviation): non-biofilm producer: OD ≤ ODc, weak biofilm producer: ODc < OD ≤ 2×ODc, moderate biofilm producer: 2×ODc < OD ≤ 4×ODc, strong biofilm producer: OD > 4×ODc.

2.5. Green Synthesis of Silver Nanoparticles Using G. glabra Root Extract

Dried *G. glabra* root was powdered, and 10 g was added to 100 mL sterile double distilled water. The mixture was heated and stirred at 60 °C for 1 hour, filtered through Whatman No. 1 paper, and stored at 4 °C (Rani et al., 2022). For AgNP synthesis, 0.01 g $AgNO_3$ was dissolved in 10 mL double distilled water and mixed with 20 mL of root extract. The mixture was heated at 80 °C until the color changed to dark brown, indicating nanoparticle formation (Alobaid et al., 2022).

2.6. Characterization of AgNPs

- **UV–Vis Spectroscopy**: Absorption spectra were recorded between 200–700 nm (Cary 100, Australia).
- **SEM/EDS**: Surface morphology and elemental composition were analyzed using SEM (CamScan MV2300) coupled with EDS (S3700N).
- **XRD**: Crystalline structure and particle size were determined using Philips PW1373 X-ray diffractometer.
- **FTIR**: Functional groups involved in nanoparticle stabilization were analyzed by FTIR (Shimadzu) over the range 400–4000 cm^{-1}.

2.7. Antibacterial Activity of AgNPs

2.7.1. Well Diffusion Method

The antimicrobial activity of AgNPs was evaluated using the agar well diffusion method (Goda et al., 2022). Mueller–Hinton agar plates were inoculated with 0.5 McFarland MDR-*P. aeruginosa* suspensions. Wells (6 mm) were filled with 50 µL of AgNPs at concentrations of 1500-100 µg/mL. Plates were incubated at 37 °C overnight, and zones of inhibition were measured.

2.7.2. MIC and MBC

MICs were determined using broth microdilution in 96-well plates. AgNPs were serially diluted (500-0.97 µg/mL) in nutrient broth. Each well received 100 µL of diluted MDR-*P. aeruginosa* suspension and 100 µL of AgNPs. Plates were incubated at 37 °C for 24 hours. MBC was determined by subculturing 10 µL from wells without visible growth onto nutrient agar. The lowest concentration with no visible colony formation was recorded as the MBC (Singh et al., 2018).

2.8. Antibiofilm Activity of AgNPs

2.8.1. Biofilm Inhibition Assay

Biofilm inhibition was evaluated using the microtiter plate method. Diluted bacterial suspensions (100 µL) were mixed with 100 µL of AgNPs (500-0.97 µg/mL) and incubated at 37 °C for 24–48 hours. Wells were washed with PBS, air dried, stained with 0.1% safranin, and solubilized in ethanol. OD was measured at 492 nm (Chegini et al., 2024).

2.8.2. Biofilm Eradication Assay

Mature biofilms were formed in microplates by incubating bacterial suspensions for 24–48 h. After washing to remove planktonic cells, 100 µL of AgNPs (500-0.97 µg/mL) were added and incubated again for 24 h. Biofilm quantification followed the same staining and OD measurement protocol (Aflakian and Hashemitabar, 2025).

2.8.3. Biofilm Inhibition/Eradication %

Biofilm inhibition or eradication was calculated using the formula (El-Telbany and El-Sharaki, 2022):

% Inhibition/Eradication = [1 – (OD test / OD control)] × 100

2.9. Ethical Considerations

The study received ethical clearance from the Scientific Committee of the Biology Department at Soran University. Verbal consent was obtained from all participating patients prior to sample collection.

2.10. Data Analysis

All experimental data were analyzed using Microsoft Excel (Microsoft Office LTSC Professional Plus 2021) and OriginPro 2025 (64-bit, SRI 10.2.0.196). Descriptive statistics, including mean and standard deviation, were calculated for triplicate measurements to ensure reproducibility and reliability.

3. Results

3.1. Bacterial Isolation and Identification

Samples were collected from different clinical sources, including burn wounds, surgical wounds, sputum, urine, and ear swabs. Out of 128 samples, 34 isolates (26.6%) were identified as *P. aeruginosa* based on growth on cetrimide agar, colony morphology, gram staining, oxidase test, and confirmation using the VITEK2 system. The distribution was as follows: sputum (7 isolates), urine (9), burn wounds (7), surgical wounds (8), and ear swabs (3).

3.2. Antimicrobial susceptibility testing

The disc diffusion experiment was used to assess the sensitivity of each *P. aeruginosa* isolate (34) to various antibiotics. The results were classified as resistant (R), intermediate (I), or sensitive (S) isolates based on the diameter of the inhibitory zone, in accordance with the clinical breakpoints established by the (Clinical and Laboratory Standards Institute, 2020). The emergence of resistance in *P. aeruginosa* to numerous antimicrobial drugs poses a significant difficulty in managing its infections. The prevalence of resistance varied according to the specific antibacterial agent examined with rates ranging from 23% to 97% among the tested isolates, figure (1). The resistance for each Imipenem-IPM, Ciprofloxacin-CIP, Gentamicin-GEN, Tobramycin-TOB, and Piperacillin–Tazobactam-TPZ is around 23.5%. The resistance levels for Amikacin-AK and Meropenem-MR are 26.4%, whereas the resistance levels for Ceftazidime-CAZ, Aztreonam-AZT, Cefotaxime-CTX, and Doxycycline-DO are 73.5%, 85.29%, 88.23%, and 97%, respectively. Ultimately, 26 (76.5%) strains demonstrated resistance to a minimum of three classes of antimicrobials, categorizing them as MDR-*P. aeruginosa*.

3.3. Biofilm formation

In this study, the biofilm-forming ability of multidrug-resistant (MDR) *P. aeruginosa* isolates was assessed using the microtiter plate method figure 2 (A). The result showed 80.8% strong, 11.5% moderate, and 3.85%weak, 3.85% no biofilm formation ability, figure 2 (B).

3.4. Nanoparticle characterization

3.4.1. UV–Visible Spectroscopy

The alteration in solution color to dark brown served as an early visual clue for AgNP creation, whereas UV–Visible spectroscopy was utilized as a precise analytical method to observe and verify the synthesis process. The UV–Visible absorption spectrum of AgNPs synthesized with *G. glabra* root extract had a significant surface plasmon resonance (SPR) peak at 424.1 nm figure 3 (A).

3.4.2 X-ray Diffraction (XRD)

XRD patterns exhibited distinct peaks at 2θ values of 37.4987°, 43.6996°, and 63.9524°, which correspond to the (111), (200), and (220) planes of the face-centered cubic (FCC) structure of silver, respectively figure 3 (B). These findings correspond with the standard diffraction data from JCPDS card No. 98-005-3759.

3.4.3. Fourier-Transform Infrared Spectroscopy (FTIR)

FTIR was used to discover the functional groups implicated in the production and stabilization of AgNPs figure 3 (C). The FTIR spectra of AgNPs exhibited a peak at 3119 cm^{-1}, indicative of O–H

stretching vibrations, signifying the presence of phenolic chemicals that likely facilitate nanoparticle stabilization. The peaks at 1567 cm^{-1} and 1076 cm^{-1} were ascribed to C=C stretching in aromatic rings and C–O stretching, respectively, indicating the presence of flavonoids or glycosidic chemicals. The peaks at 562 cm^{-1} and 412 cm^{-1} likely correspond to metal–oxygen stretching and Ag–O or Ag–N bonding, respectively, suggesting an interaction between silver and the functional groups present in the extract. The FTIR spectrum of the *G. glabra* root extract exhibited peaks at 773, 1032, 1317, 1614, 2933, and 3316 cm^{-1}. These related to aromatic C–H bending, C–O stretching, S=O or C–N stretching, C=C or C=O stretching, C–H stretching, and O–H stretching vibrations, which are likely essential in the reduction and stabilization processes of nanoparticle production.

3.4.4. Energy-Dispersive X-ray Spectroscopy (EDS)

The EDS analysis verified the chemical composition of the created nanoparticles figure 3 (D). Silver (Ag) was the predominant element, accompanied by measurable quantities of oxygen (O), phosphorous (P), and magnesium (Mg).

3.4.5. Scanning Electron Microscopy (SEM)

SEM analysis demonstrated that the produced AgNPs showed various morphologies, with particle diameters ranging from 49.53 to 97.14 nm figure 3 (E).

3.5. Antimicrobial activity of AgNPs by Well diffusion, MIC and MBC

The antibacterial property of the synthesized AgNPs against MDR- *P. aeruginosa* was assessed using the agar well diffusion technique. Mueller-Hinton agar plates were inoculated with an overnight culture of *P. aeruginosa* by using a sterile swab. Wells were formed by utilizing a sterile cork borer, and different concentrations of AgNPs (1500, 1000, 500, 300, and 200, 100 µg/mL) were placed into the wells. The results exhibited a concentration-dependent antibacterial effect, with inhibition zone diameters rising as the concentrations of AgNPs increased. The largest zone of inhibition, measuring 17 mm, was seen at a concentration of 1500 µg/mL. The lowest tested concentration (100 µg/mL) resulted in a zone of inhibition of 8 mm figure 4. The MIC was established as the minimum concentration of AgNPs that inhibited bacterial growth. Each *P. aeruginosa* isolate was incubated with AgNPs at concentrations ranging from 0.97 to 500 µg/mL, prepared in a series of twofold dilutions using a microplate assay. The results showed that MIC values ranged from 62.5 to 500 µg/mL among the tested samples. The MBC was defined as the minimum concentration of nanoparticles that prevented visible bacterial growth on agar plates, ranging from 62.5 to >500 µg/mL.

3.6. Antibiofilm activity of silver nanoparticles

The anti-biofilm efficacy of the synthesized AgNPs was assessed among a concentration ranges (500, 250, 125, 62.5, 32.25, 15.6, 7.8, 3.9, 1.95, 0.97 µg/mL), resulting in biofilm formation inhibition rates of (97.5%, 97.39%, 97.37%, 66%, 23%, 6%, 4%, 3%, 2.6%, 2%) figure 5 (A).

The efficacy of AgNPs in eliminating pre-formed biofilms was documented at (85%, 83%, 82%, 70%, 48%, 21%, 15%, 14%, 14%, 0.7%) figure 5 (B).

4. Discussion

The emergence of resistance in *P. aeruginosa* to numerous antimicrobial drugs poses a significant difficulty in managing its infections. This study demonstrates the prevalence of resistance varied according to the specific antibacterial agent examined with rates ranging from 23% to 97% among the tested isolates. The susceptibility testing of *P. aeruginosa* isolates to the evaluated antibiotics revealed a significant prevalence of resistance to CAZ, AZT, CTX, and DO, followed by AK, MR, IPM, CIP, GEN, TOB, and TPZ. The increased prevalence of multidrug-resistant (MDR) patterns among the bacteria in this research may be attributed to variables such as self-medication, empiric use, and the extensive prior use of a wide range of these antibiotics.

Previous research indicates a higher resistance to TPZ (75.8%), followed by CIP (34.3%) (Momenah et al., 2023). Another study reveals lower resistance rates for AZT, CTX, and CAZ at 11.76%, 82.35%, and 5.88%, respectively, with 100% sensitivity to IMP and MER, but increased resistance to TOB, GEN, and CIP at 75% (Bhuiya et al., 2018). Simultaneously, another study indicates a resistance rate of 67.9% for CAZ, while

33.3% of isolates demonstrated resistance to MR, a powerful antipseudomonal antibiotic (Haji et al., 2024).

Ultimately, 26 (76.5%) strains demonstrated resistance to a minimum of three classes of antimicrobials, categorizing them as MDR-*P. aeruginosa*. This outcome is greater than that of the MDR-*P. aeruginosa* isolates by (Yang et al., 2023), in which 29.8% of the isolates were determined to be MDR. Additionally, another study by (Haji et al., 2024) reported that 85.8% of *P. aeruginosa* isolates were MDR. The wide variation in resistance levels across various research can be linked to geographical variability, the type and quantity of samples obtained, and the differing antibiotic policies established in each country.

P. aeruginosa is a well-known biofilm-forming bacterium. Its ability to develop biofilms contributes significantly to its persistence in various infections and reduces the effectiveness of antibiotics (Ghafoor et al., 2011). The result shows 80.8 % strong biofilm producers, 11.5% moderate biofilm producers, and 3.85%weak biofilm producers, 3.85% no biofilm formation ability. A similar study reported that 65.3% of strains exhibited strong biofilm formation, while 12.8% and 21.7% showed moderate and weak biofilm-forming potential, respectively (Haji et al., 2024). These findings are also supported by (Kamer et al., 2024), who emphasized the clinical significance of biofilm formation in antibiotic resistance.

The characterization result revealed the successful green synthesis of AgNPs using *G. glabra* root extract. The UV–Vis spectroscopy peak at 424.1 nm, matches within the standard SPR range of 400–450 nm, thereby establishing the effective synthesis of AgNPs. The lack of extra peaks indicates the successful reduction of Ag^+ ions and stabilizing by phytochemicals in the extract. The absorption band at a matching wavelength indicating the presence of nanosilver was also reported by (Kambale et al., 2020). XRD analysis detected lack of secondary peaks signifies that the synthesized nanoparticles are phase-pure metallic silver. The mean crystallite size, determined via the Scherrer equation, was 18.92 nm. The study indicates that the crystallite size of green silver nanoparticles was determined to be 21.26 nm (Juzer et al., 2025). FTIR detected the role of flavonoids, phenolic compounds, and glycosides, which are likely essential in the reduction and stabilization processes of nanoparticle production (Kambale et al., 2020). EDS analyses elemental composition that is detect robust Ag signal at about 2.98 keV corroborated the reduction of silver ions to their metallic state (Ag^0), enhanced by the phytochemicals in the *G. glabra* root extract, matching the results by (Dybkova et al., 2024), also SEM showed, a certain level of aggregation was noted, usually related to green synthesis techniques due to the various properties of biomolecules serving as reducing and capping agents (Cifuentes-Jiménez et al., 2024).

Antimicrobial activity of AgNPs by well diffusion exhibited a concentration-dependent antibacterial effect, with inhibition zone diameters rising as the concentrations of AgNPs increased. Zone of inhibition, measuring between (8-17 mm). The results indicate that the synthesized AgNPs have considerable antibacterial efficacy against MDR-*P. aeruginosa*. The findings of the present study align with those of a recent investigation that documented the antibacterial efficacy of green AgNPs (Goda et al., 2022). Additionally, (Huq and Akter, 2021) found that the diameters of the AgNPs' zone inhibition against *P. aeruginosa* were 24.7 mm.

MIC ranging between (62.5 -500 µg/mL), while the MBC ranging between (62.5 to >500 µg/mL). The result is greater than that of (Huq and Akter, 2021) study, wherein green synthesis AgNPs exhibited a MIC of 12.5 µg/mL and an MBC of 25 µg/mL for *P. aeruginosa*. Various theories have been proposed on the mechanism by which AgNPs exert their antibacterial effects on microorganisms. Initially, they adhere to and puncture bacterial cell walls, resulting in structural damage and elevated membrane permeability, potentially leading in cell death (Sondi and Salopek-Sondi, 2004). Secondly, AgNPs can penetrate cells and interact with Sulphur- and phosphorus-containing molecules such as DNA and proteins, thereby altering their functions and triggering oxidative stress through the production of reactive oxygen species (ROS). The release of silver ions from the nanoparticles, which because of their size and

charge can interact with cellular components to modify metabolic pathways, membranes, and even genetic material, is a third mechanism occurring simultaneously with both previously described mechanism (Anees Ahmad et al., 2020).

This research demonstrated that AgNPs significantly inhibited the adhesion and formation of biofilms by the examined *P. aeruginosa* strains in a dosage-dependent manner. The result showed in concentration 62.5 µg/mL *P. aeruginosa* have ability to biofilm inhibition (66%). Research indicates that the percentage of biofilm inhibition varied from 2% to 89% at 0.5 MIC (2.65 to 21.25 µg/mL) (Kamer et al., 2024). Another study illustrates that *Terminalia catappa* capped AgNPs exhibit biofilm inhibition percentages of 58.70 ± 0.8%, 65.6 ± 1.5%, 66.4 ± 0.9%, and 75.14 ± 1.3% against MDR-*P. aeruginosa* at concentrations of 0.95, 1.95, 3.90, and 7.80 µg/mL after 24 hours of treatment, respectively (Ansari et al., 2021). Also, result showed biofilm eradication (70%) at concentration 62.5 µg/mL. This corresponds with another study indicating that AgNPs reduced biofilm biomass. The biggest eradication rates were recorded at concentrations of 1 mg/mL and 2 mg/mL, yielding 44% and 36% in *P. aeruginosa*, respectively (Skóra et al., 2021). Similarly, AgNPs biosynthesized from *Peganum harmala* seed extract eradicated *P. aeruginosa* biofilms. Significant biomass, metabolic, and quorum-sensing gene expression reductions (Al-Momani et al., 2023). Another study revealed that Seabuckthorn-derived AgNPs eliminated *P. aeruginosa* immature and mature biofilms (Gondil et al., 2019).

The results demonstrate that the synthesized AgNPs are effective in both inhibiting biofilm development and destroying established biofilms. Certain studies indicate that the primary mechanism of biofilm eradication involves the adhesion of AgNPs to the exopolysaccharide matrix, which disrupts the biofilm structure by targeting the peptidoglycan structure in bacterial cell membranes, resulting in physical damage, ion release, and ROS generation, resulting in oxidative stress and DNA damage (Bala Subramaniyan et al., 2020).

5. Conclusion

This study successfully demonstrated the green synthesis of AgNPs using *G. glabra* root extract and evaluated their antibacterial and antibiofilm activities against MDR-*P. aeruginosa* clinical isolates. *G. glabra* is a commonly utilized traditional medicinal herb, recognized worldwide for its efficacy in treating various diseases and its rich supply of bioactive compounds that facilitate nanoparticle production. The findings highlight the promising potential of plant-mediated AgNPs as a cost-effective and eco-friendly alternative to conventional antibiotics for managing MDR bacterial infections and biofilm-associated complications. However, further in vivo studies and clinical validation are necessary to translate these results into practical therapeutic applications.

Conflict of Interest

The author declares that there are no financial, personal, or institutional conflicts of interest related to the content of this manuscript.

Acknowledgments

The author sincerely thanks the Biology Department, Faculty of Science, Soran University, for their academic support and encouragement throughout this research. Deep appreciation is also extended to the Scientific Research Center at Soran University for providing access to laboratory facilities and resources that made this work possible. The author also gratefully acknowledges the Faculty of Science, Salahaddin University, for their valuable support and collaboration during the course of this study.

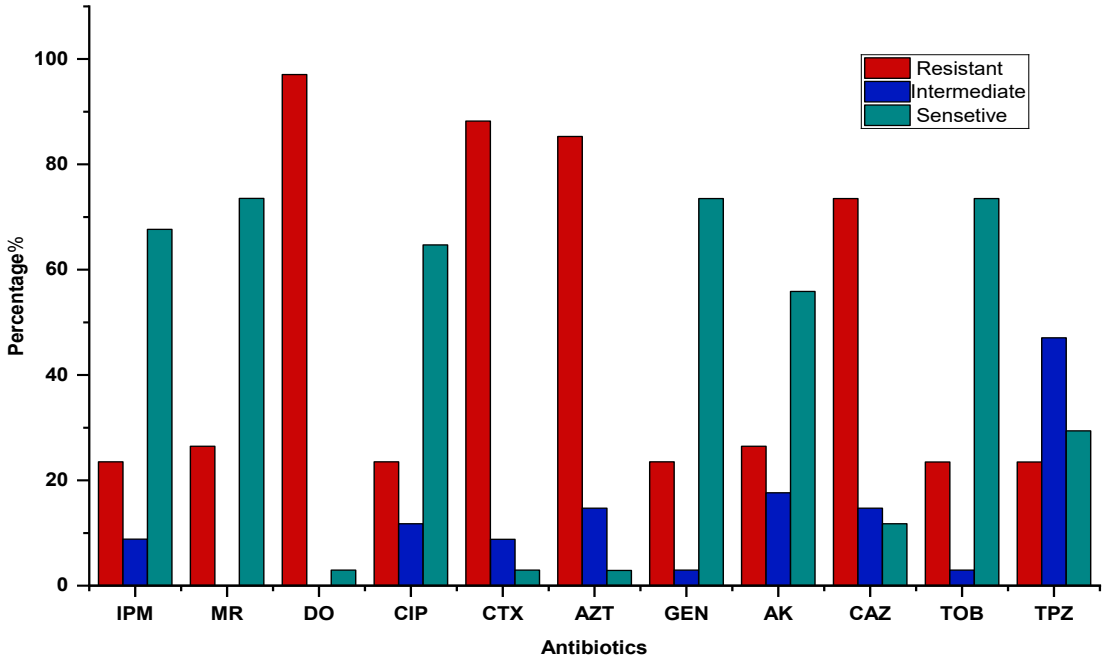

Figure.1 Prevalence of resistance among *P. aeruginosa* isolates to several antibiotics, Imipenem 10 µg (IPM), Meropenem 10 µg (MR), Doxycycline 30 µg (DO), Ciprofloxacin 5 µg (CIP), Cefotaxime 30 µg (CTX), Aztreonam 30 µg (AZT), Gentamicin 10 µg (GEN), Amikacin 30 µg (AK), Ceftazidime 30 µg (CAZ), Tobramycin 10 µg (TOB), Piperacillin-Tazobactam 100/10 µg (TPZ).

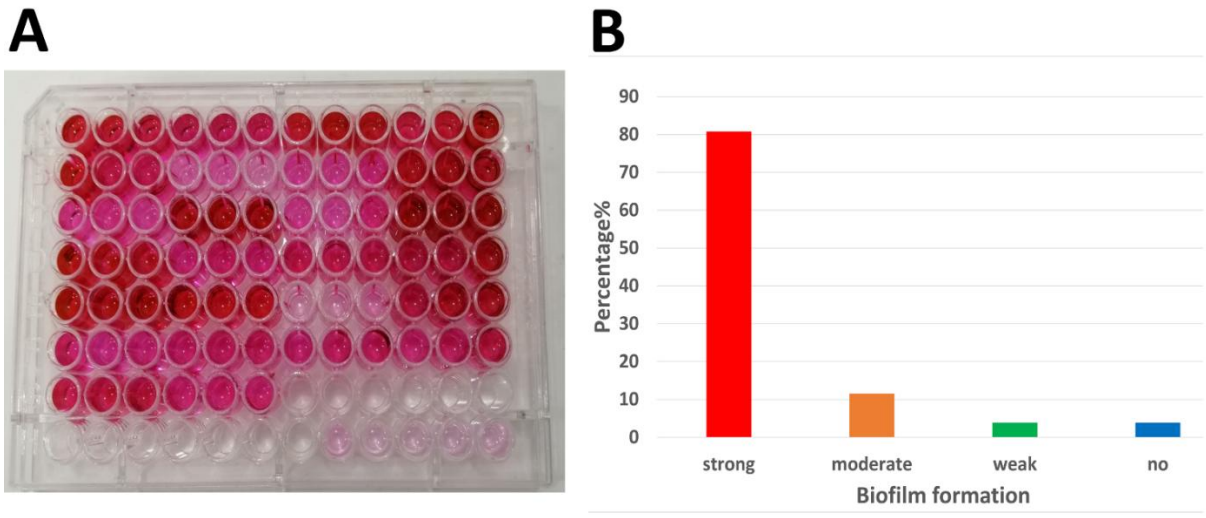

Figure. **2** Biofilm-forming ability among multidrug-resistant *P. aeruginosa* isolates.
(A) Safranin-stained 96-well microtiter plate showing varying intensities of biofilm formation. Dark red wells indicate strong biofilm producers, while pale or clear wells represent moderate, weak or non-biofilm producers. (B) Distribution of biofilm production based on OD_{492} values: strong (OD > 0.36), moderate (0.18 < OD ≤ 0.36), weak (OD ≤ 0.18), and non-producers (OD ≤ 0.09). Among the tested isolates, 80.8% were strong biofilm producers, followed by 11.5% moderate, 3.5% weak, and 3.5% non-producers.

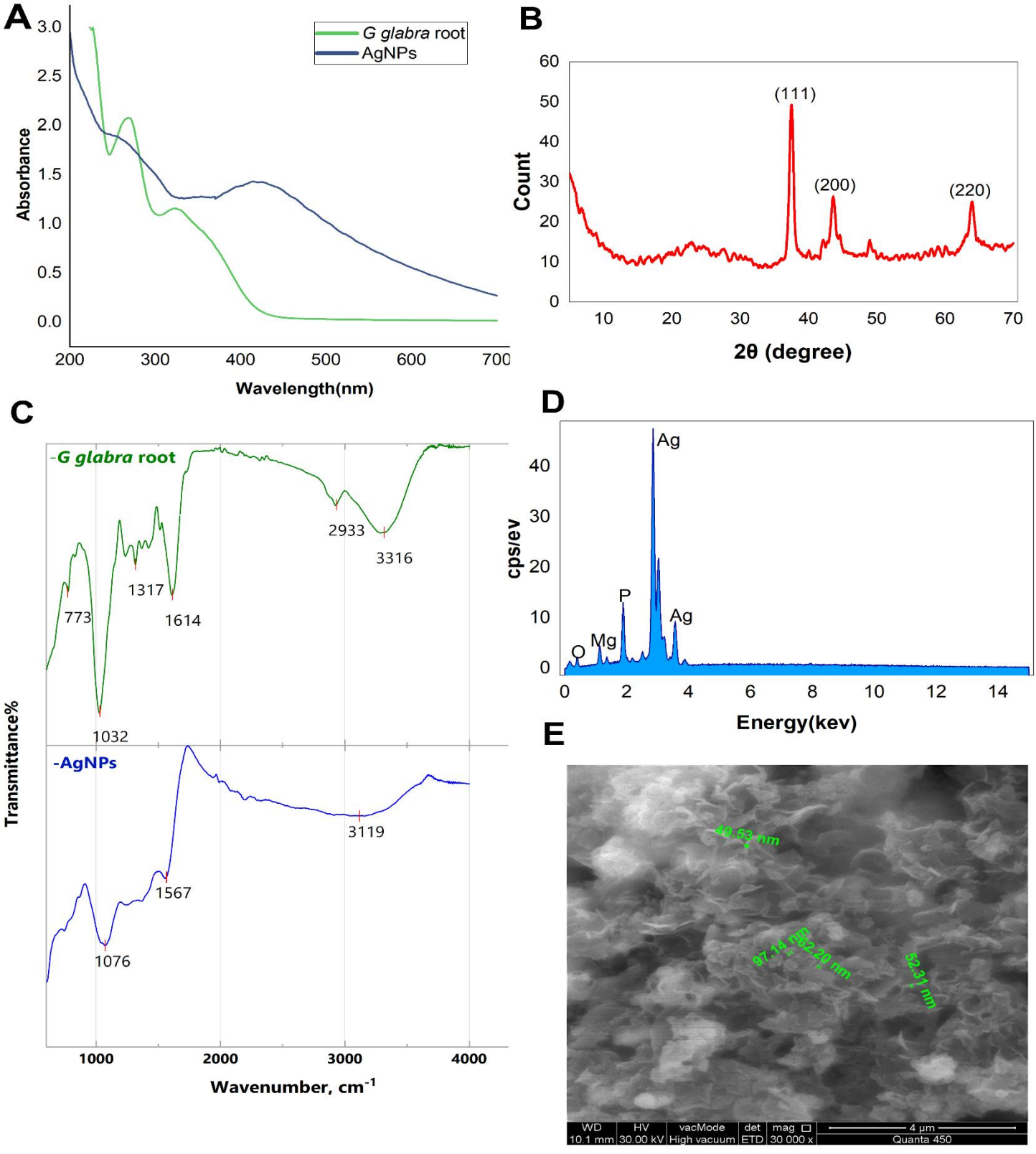

Figure. 3 Characterization of AgNPs **A-** UV-vis spectroscopy **B-** XRD result **C-** FTIR analysis **D-** EDS analysis **E-** SEM result.

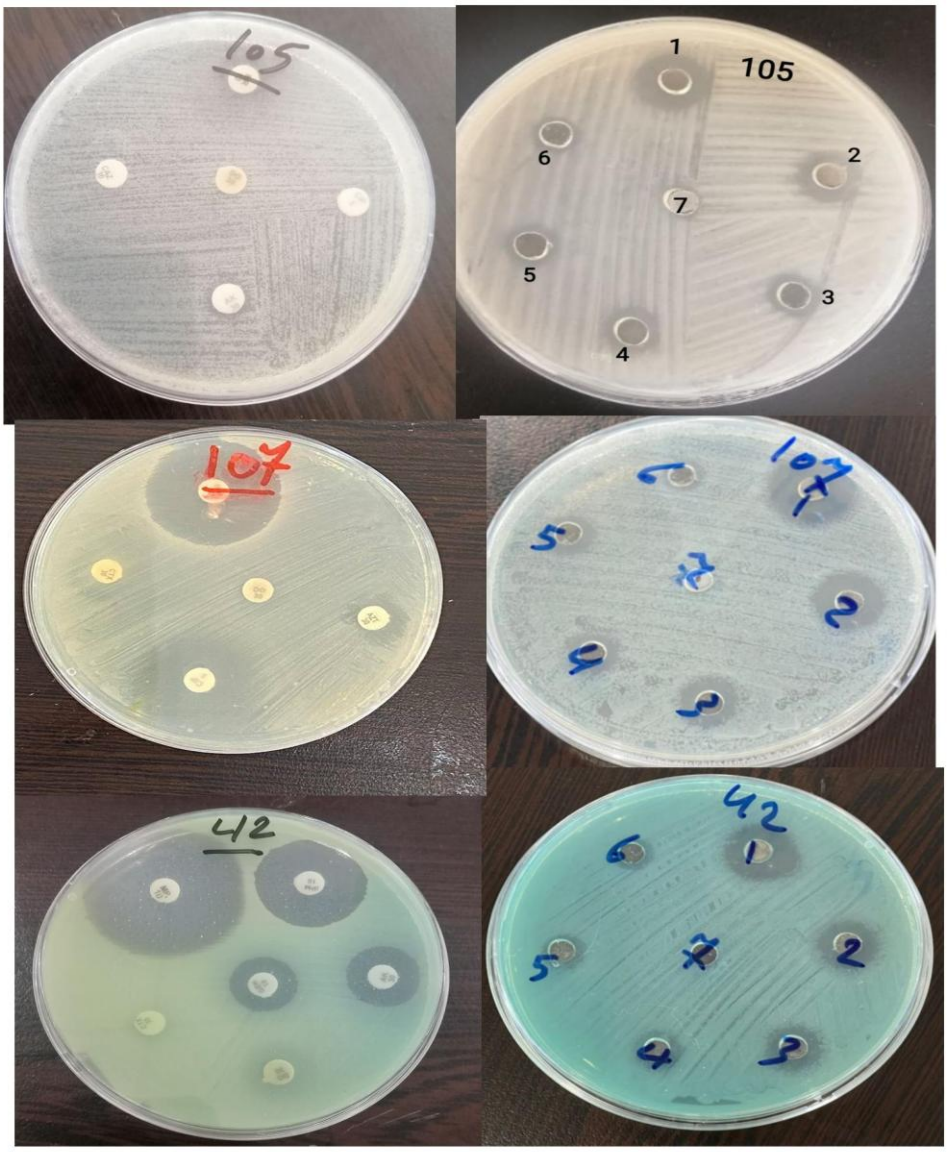

Figure. 4 Antibacterial activity of biosynthesized AgNPs against MDR-*P. aeruginosa* isolates, evaluated by the agar well diffusion method. Each Petri dish corresponds to a distinct clinical isolate (sample numbers 42, 105, and 107). Wells 1–6 were loaded with AgNPs at concentrations ranging from 1500 to 100 µg/mL, while well 7 served as the negative control containing double-distilled water. Zones of inhibition were measured after 24 hours of incubation at 37 °C, with the maximum observed diameter reaching 17 mm.

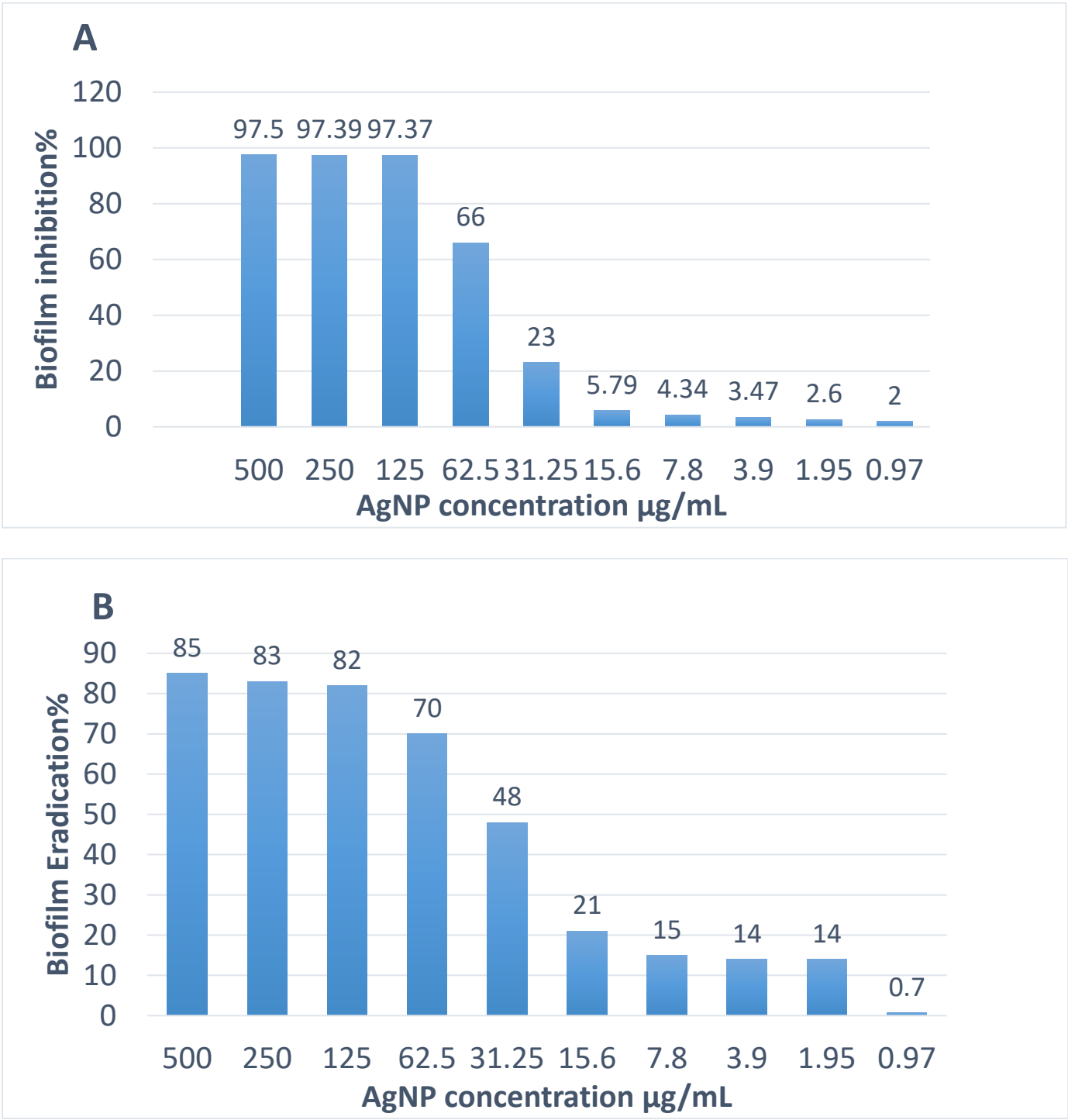

Figure.5 Percentage of biofilm inhibition(A) and biofilm eradication(B) activity of varying concentrations of AgNPs against MDR-*P. aeruginosa*, assessed using the microplate assay. A concentration-dependent manner was observed.

References

Abdulhaq, N., Nawaz, Z., Zahoor, M. A. & Siddique, A. B. 2020. Association of biofilm formation with multi drug resistance in clinical isolates of *Pseudomonas aeruginosa*. *Excli j,* 19**,** 201-208.

Aflakian, F. & Hashemitabar, G. 2025. Biosynthesized silver nanoparticles at subinhibitory concentrations as inhibitors of quorum sensing, pathogenicity, and biofilm formation in *Pseudomonas aeruginosa* PAO1. *Heliyon,* 11.

Afrasiabi, S. & Partoazar, A. 2024. Targeting bacterial biofilm-related genes with nanoparticle-based strategies. *Front Microbiol,* 15**,** 1387114.

Al-Momani, H., Almasri, M., Al Balawi, D. A., Hamed, S., Albiss, B. A., Aldabaibeh, N., Ibrahim, L., Albalawi, H., Al Haj Mahmoud, S., Khasawneh, A. I., Kilani, M., Aldhafeeri, M., Bani-Hani, M., Wilcox, M., Pearson, J. & Ward, C. 2023. The efficacy of biosynthesized silver nanoparticles against *Pseudomonas aeruginosa* isolates from cystic fibrosis patients. *Scientific Reports,* 13**,** 8876.

Alobaid, H. M., Daghestani, M. H., AL-Malahi, N. M., Alzahrani, S. A., Hassen, L. M. & Metwally, D. M. 2022. Exploring the effect of silver nanoparticles on gene expression in colon cancer cell line HCT116. *Green Processing and Synthesis,* 11**,** 1108-1117.

Anees Ahmad, S., Sachi Das, S., Khatoon, A., Tahir Ansari, M., Afzal, M., Saquib Hasnain, M. & Kumar Nayak, A. 2020. Bactericidal activity of silver nanoparticles: A mechanistic review. *Materials Science for Energy Technologies,* 3**,** 756-769.

Ansari, M. A., Kalam, A., Al-Sehemi, A. G., Alomary, M. N., AlYahya, S., Aziz, M. K., Srivastava, S., Alghamdi, S., Akhtar, S., Almalki, H. D., Adil, S. F., Khan, M. & Hatshan, M. R. 2021. Counteraction of Biofilm Formation and Antimicrobial Potential of *Terminalia catappa* Functionalized Silver Nanoparticles against *Candida albicans* and Multidrug-Resistant Gram-Negative and Gram-Positive Bacteria. *Antibiotics,* 10**,** 725.

Antunes, L. C. M., Ferreira, R. B. R., Buckner, M. M. C. & Finlay, B. B. 2010. Quorum sensing in bacterial virulence. *Microbiology,* 156**,** 2271-2282.

Azam, M. W. & Khan, A. U. 2019. Updates on the pathogenicity status of *Pseudomonas aeruginosa*. *Drug Discovery Today,* 24**,** 350-359.

Bala Subramaniyan, S., Senthilnathan, R., Arunachalam, J. & Anbazhagan, V. 2020. Revealing the Significance of the Glycan Binding Property of *Butea monosperma* Seed Lectin for Enhancing the Antibiofilm Activity of Silver Nanoparticles against Uropathogenic *Escherichia coli*. *Bioconjugate Chemistry,* 31**,** 139-148.

Bauer, A. W., Kirby, W. M. M., Sherris, J. C. & Turck, M. 1966. Antibiotic Susceptibility Testing by a Standardized Single Disk Method. *American Journal of Clinical Pathology,* 45**,** 493-496.

Bhuiya, M., Sarkar, M. K. I., Sohag, M. H., Ali, H., Roy, C. K., Akther, L. & Sarker, A. F. 2018. Enumerating Antibiotic Susceptibility Patterns of *Pseudomonas aeruginosa* Isolated from Different Sources in Dhaka City. *The Open Microbiology Journal,* 12**,** 172-180.

Brindhadevi, K., LewisOscar, F., Mylonakis, E., Shanmugam, S., Verma, T. N. & Pugazhendhi, A. 2020. Biofilm and Quorum sensing mediated pathogenicity in *Pseudomonas aeruginosa*. *Process Biochemistry,* 96**,** 49-57.

Chegini, Z., Shariati, A., Alikhani, M. Y., Safaiee, M., Rajaeih, S., Arabestani, M. & Azizi, M. 2024. Antibacterial and antibiofilm activity of silver nanoparticles stabilized with C-phycocyanin against drug-resistant *Pseudomonas aeruginosa* and *Staphylococcus aureus*. *Front Bioeng Biotechnol,* 12**,** 1455385.

Chimi, L. Y., Noubom, M., Bisso, B. N., Singor Njateng, G. S. & Dzoyem, J. P. 2024. Biofilm Formation, Pyocyanin Production, and Antibiotic Resistance Profile of *Pseudomonas aeruginosa* Isolates from Wounds. *International Journal of Microbiology,* 2024**,** 1207536.

Cifuentes-Jiménez, C., Bolaños-Carmona, M. V., Enrich-Essvein, T., Rodríguez-Navarro, A. B., González-López, S., Yamauti, M. & Álvarez-Lloret, P. 2024. Green synthesis of chitosan- and fluoride-functionalized silver nanoparticles using *Camellia sinensis*: Characterization and dental applications. *International Journal of Biological Macromolecules,* 268**,** 131676.

Clinical and Laboratory Standards Institute 2020. Performance Standards for Antimicrobial Susceptibility Testing. 30th ed. Wayne, PA: CLSI.

Das, M. C., Sandhu, P., Gupta, P., Rudrapaul, P., De, U. C., Tribedi, P., Akhter, Y. & Bhattacharjee, S. 2016. Attenuation of *Pseudomonas aeruginosa* biofilm formation by Vitexin: A combinatorial study with azithromycin and gentamicin. *Scientific Reports,* 6**,** 23347.

Dybkova, S., Goncharuk, O., Rieznichenko, L., Terpiłowski, K., Borysenko, L., Gruzina, T., Dybkova, K. & Szewczuk-Karpisz, K. 2024. Aqueous dispersions of 'green' silver nanoparticles for eco-applications: Synthesis, structure and biosafety. *Journal of Molecular Liquids,* 415**,** 126319.

El-Telbany, M. & El-Sharaki, A. 2022. Antibacterial and anti-biofilm activity of silver nanoparticles on multi-drug resistance *pseudomonas aeruginosa* isolated from dental-implant. *Journal of Oral Biology and Craniofacial Research,* 12**,** 199-203.

Fernebro, J. 2011. Fighting bacterial infections—Future treatment options. *Drug Resistance Updates,* 14**,** 125-139.

Ghafoor, A., Hay, I. D. & Rehm, B. H. 2011. Role of exopolysaccharides in *Pseudomonas aeruginosa* biofilm formation and architecture. *Appl Environ Microbiol,* 77**,** 5238-46.

Goda, R. M., El-Baz, A. M., Khalaf, E. M., Alharbi, N. K., Elkhooly, T. A. & Shohayeb, M. M. 2022. Combating Bacterial Biofilm Formation in Urinary Catheter by Green Silver Nanoparticle. *Antibiotics* 11**,** 495.

Gondil, V. S., Kalaiyarasan, T., Bharti, V. K. & Chhibber, S. 2019. Antibiofilm potential of Seabuckthorn silver nanoparticles (SBT@AgNPs) against *Pseudomonas aeruginosa*. *3 Biotech,* 9**,** 402.

Gusso, B. P., Almeida, A. R., Nunes, M. R., Becker, D., Hotza, D., da Rosa, C. G., dos Santos, V. V. & da Silva, B. F. 2025. The Antimicrobial Activity of Silver

Nanoparticles Biosynthesized Using *Cymbopogon citratus* Against Multidrug-Resistant Bacteria Isolated from an Intensive Care Unit. *Pharmaceuticals,* 18**,** 1120.

Haji, S. H., Ganjo, A. R., Faraj, T. A., Fatah, M. H. & Smail, S. B. 2024. The enhanced antibacterial and antibiofilm properties of titanium dioxide nanoparticles biosynthesized by multidrug-resistant *Pseudomonas aeruginosa*. *BMC Microbiology,* 24**,** 379.

Hetta, H. F., Ramadan, Y. N., Al-Harbi, A. I., A. Ahmed, E., Battah, B., Abd Ellah, N. H., Zanetti, S. & Donadu, M. G. 2023. Nanotechnology as a Promising Approach to Combat Multidrug Resistant Bacteria: A Comprehensive Review and Future Perspectives. *Biomedicines,* 11**,** 413.

Huq, M. A. & Akter, S. 2021. Bacterial Mediated Rapid and Facile Synthesis of Silver Nanoparticles and Their Antimicrobial Efficacy against Pathogenic Microorganisms. *Materials (Basel),* 14.

Juzer, T., Soundharajan, R. & Srinivasan, H. 2025. *Camellia sinensis* mediated silver nanoparticles: eco-friendly antimicrobial agent to control multidrug resistant Gram-positive *Staphylococcus aureus*. *Discover Nano,* 20**,** 92.

Kambale, E. K., Nkanga, C. I., Mutonkole, B.-P. I., Bapolisi, A. M., Tassa, D. O., Liesse, J.-M. I., Krause, R. W. M. & Memvanga, P. B. 2020. Green synthesis of antimicrobial silver nanoparticles using aqueous leaf extracts from three Congolese plant species (*Brillantaisia patula*, *Crossopteryx febrifuga* and *Senna siamea*). *Heliyon,* 6.

Kamer, A. M. A., El Maghraby, G. M., Shafik, M. M. & Al-Madboly, L. A. 2024. Silver nanoparticle with potential antimicrobial and antibiofilm efficiency against multiple drug resistant, extensive drug resistant *Pseudomonas aeruginosa* clinical isolates. *BMC Microbiology,* 24**,** 277.

Khan, J., Tarar, S. M., Gul, I., Nawaz, U. & Arshad, M. 2021. Challenges of antibiotic resistance biofilms and potential combating strategies: a review. *3 Biotech,* 11**,** 169.

Magiorakos, A. P., Srinivasan, A., Carey, R. B., Carmeli, Y., Falagas, M. E., Giske, C. G., Harbarth, S., Hindler, J. F., Kahlmeter, G., Olsson-Liljequist, B., Paterson, D. L., Rice, L. B., Stelling, J., Struelens, M. J., Vatopoulos, A., Weber, J. T. & Monnet, D. L. 2012. Multidrug-resistant, extensively drug-resistant and pandrug-resistant bacteria: an international expert proposal for interim standard definitions for acquired resistance. *Clin Microbiol Infect,* 18**,** 268-81.

Makabenta, J. M. V., Nabawy, A., Li, C. H., Schmidt-Malan, S., Patel, R. & Rotello, V. M. 2021. Nanomaterial-based therapeutics for antibiotic-resistant bacterial infections. *Nature Reviews Microbiology,* 19**,** 23-36.

Mikhailova, E. O. 2025. Green Silver Nanoparticles: An Antibacterial Mechanism. *Antibiotics,* 14**,** 5.

Momenah, A. M., Bakri, R. A., Jalal, N. A., Ashgar, S. S., Felemban, R. F., Bantun, F., Hariri, S. H., Barhameen, A. A., Faidah, H. & Al-Said, H. M. 2023. Antimicrobial Resistance Pattern of *Pseudomonas aeruginosa*: An 11-Year Experience in a Tertiary Care Hospital in Makkah, Saudi Arabia. *Infect Drug Resist,* 16**,** 4113-4122.

Pastorino, G., Cornara, L., Soares, S., Rodrigues, F. & Oliveira, M. 2018. Liquorice (*Glycyrrhiza glabra*): A phytochemical and pharmacological review. *Phytother Res,* 32**,** 2323-2339.

Rajivgandhi, G. N., Ramachandran, G., Maruthupandy, M., Manoharan, N., Alharbi, N. S., Kadaikunnan, S., Khaled, J. M., Almanaa, T. N. & Li, W.-J. 2020. Anti-oxidant, anti-bacterial and anti-biofilm activity of biosynthesized silver nanoparticles using *Gracilaria corticata* against biofilm producing *K. pneumoniae*. *Colloids and Surfaces A: Physicochemical and Engineering Aspects,* 600**,** 124830.

Rani, K., Devi, N., Banakar, P., Kharb, P. & Kaushik, P. 2022. Nematicidal Potential of Green Silver Nanoparticles Synthesized Using Aqueous Root Extract of *Glycyrrhiza glabra*. *Nanomaterials,* 12**,** 2966.

Singh, P., Pandit, S., Garnæs, J., Tunjic, S., Mokkapati, V. R. S. S., Sultan, A., Thygesen, A., Mackevica, A., Mateiu, R. V., Daugaard, A. E., Baun, A. & Mijakovic, I. 2018. Green synthesis of gold and silver nanoparticles from *Cannabis sativa* (industrial hemp) and their capacity for biofilm inhibition. *International Journal of Nanomedicine,* 13**,** 3571-3591.

Skóra, B., Krajewska, U., Nowak, A., Dziedzic, A., Barylyak, A. & Kus-Liśkiewicz, M. 2021. Noncytotoxic silver nanoparticles as a new antimicrobial strategy. *Scientific Reports,* 11.

Sondi, I. & Salopek-Sondi, B. 2004. Silver nanoparticles as antimicrobial agent: a case study on *E. coli* as a model for Gram-negative bacteria. *Journal of Colloid and Interface Science,* 275**,** 177-182.

Thi, M. T. T., Wibowo, D. & Rehm, B. H. A. 2020. *Pseudomonas aeruginosa* Biofilms. *Int J Mol Sci,* 21.

Tuon, F. F., Dantas, L. R., Suss, P. H. & Tasca Ribeiro, V. S. 2022. Pathogenesis of the *Pseudomonas aeruginosa* Biofilm: A Review. *Pathogens,* 11.

Wu, L., Ma, T., Zang, C., Xu, Z., Sun, W., Luo, H., Yang, M., Song, J., Chen, S. & Yao, H. 2024. Glycyrrhiza, a commonly used medicinal herb: Review of species classification, pharmacology, active ingredient biosynthesis, and synthetic biology. *Journal of Advanced Research*.

Yang, A. F., Huang, V., Samaroo-Campbell, J. & Augenbraun, M. 2023. Multi-drug resistant *Pseudomonas aeruginosa*: a 2019–2020 single center retrospective case control study. *Infection Prevention in Practice,* 5**,** 100296.